

# Fiber Bundle model with Highly Disordered Breaking Thresholds

Chandreyee Roy, Sumanta Kundu and S. S. Manna\*

*Satyendra Nath Bose National Centre for Basic Sciences, Block-JD, Sector-III, Salt Lake, Kolkata-700098, India*

We present a study of the fiber bundle model using equal load sharing dynamics where the breaking thresholds of the fibers are drawn randomly from a power law distribution of the form  $p(b) \sim b^{-1}$  in the range  $10^{-\beta}$  to  $10^{\beta}$ . Tuning the value of  $\beta$  continuously over a wide range, the critical behavior of the fiber bundle has been studied both analytically as well as numerically. Our results are: (i) The critical load  $\sigma_c(\beta, N)$  for the bundle of size  $N$  approaches its asymptotic value  $\sigma_c(\beta)$  as  $\sigma_c(\beta, N) = \sigma_c(\beta) + AN^{-1/\nu(\beta)}$  where  $\sigma_c(\beta)$  has been obtained analytically as  $\sigma_c(\beta) = 10^{\beta}/(2\beta e \ln 10)$  for  $\beta \geq \beta_u = 1/(2 \ln 10)$ , and for  $\beta < \beta_u$  the weakest fiber failure leads to the catastrophic breakdown of the entire fiber bundle, similar to brittle materials, leading to  $\sigma_c(\beta) = 10^{-\beta}$ ; (ii) the fraction of broken fibers right before the complete breakdown of the bundle has the form  $1 - 1/(2\beta \ln 10)$ ; (iii) the distribution  $D(\Delta)$  of the avalanches of size  $\Delta$  follows a power law  $D(\Delta) \sim \Delta^{-\xi}$  with  $\xi = 5/2$  for  $\Delta \gg \Delta_c(\beta)$  and  $\xi = 3/2$  for  $\Delta \ll \Delta_c(\beta)$ , where the crossover avalanche size  $\Delta_c(\beta) = 2/(1 - e10^{-2\beta})^2$ .

PACS numbers: 64.60.Ht 62.20.M- 02.50.-r 05.40.-a

## 1. INTRODUCTION

Natural disasters like land slide, mine collapse, earthquake cause great losses in human lives and property. It is therefore primarily important to understand the underlying mechanisms of the failure processes so that the losses can be minimized by providing a precursor. Similarly for engineers the strength of material is a major quantity in order to make huge constructions like bridges, buildings etc. Due to these standing requirements, during the last two decades, huge amounts of scientific efforts have been invested to explore the microscopic mechanism and rupture process of disordered materials. It has been revealed that the disorder plays a crucial role in determining the strength of material and also in the fracturing process [1–5].

Models of materials in the form of a bundle consisting of a large number of parallel massless elastic fibers are well known to be simple examples of critical systems exhibiting non-trivial breakdown properties [1–5]. These systems are called the Fiber Bundle Models (FBM) where individual fibers have randomly distributed breaking thresholds. Typically, on increasing the externally applied load  $\sigma$  per fiber, the entire fiber bundle fails at a critical load  $\sigma_c$  per fiber. It is also known that for  $\sigma < \sigma_c$ , larger the external load, more extensive is the response of the system in terms of the number of fiber failures. This number diverges as  $\sigma \rightarrow \sigma_c$  from below and for  $\sigma$  beyond  $\sigma_c$  all fibers eventually fail with certainty. Therefore,  $\sigma_c$  is looked upon as the transition point from a local to the global failure of the bundle [6].

In the fiber bundle model a set of  $N$  parallel fibers is clamped at one end and an external load is applied at the other end [7, 8]. Every fiber  $i$  has its own breaking threshold  $b_i$ . If the tensile stress acting through it exceeds  $b_i$  it breaks. Random numbers  $\{b_i\}$  are drawn from a probability distribution  $p(b)$  and they are assigned as the breaking thresholds of the individual fibers whose

cumulative distribution is  $P(b) = \int_0^b p(z)dz$ .

In many FBMs, stress is treated as a conserved quantity. During the failure of an individual fiber the stress is released and it gets distributed among the remaining intact fibers. Depending on how the released stress is distributed among the intact fibers there exists various models in the literature. Among these FBMs the Equal Load Sharing (ELS) model is the most well known [8–10]. Here the released stress is distributed equally among all the remaining intact fibers. Most of the results of this model have been calculated analytically and also this model is computationally easier to tackle. On the other hand in the Local Load Sharing (LLS) model, the released stress is distributed equally only to the nearest surviving neighbors [11, 12]. In the LLS model, most of the results have been obtained numerically. A fiber is strained when some amount of stress acts through it. For ELS, the clamps at two ends of the bundle may be treated as infinitely stiff and therefore under a certain applied load, all fibers are strained by equal amounts and consequently the magnitudes of the stresses acting through the intact fibers are also equal. On the other hand, if the clamps are elastic, different fibers are strained differently and their stress values are also different as is the situation in the LLS model. A third model, intermediate between ELS and LLS, has also been considered in the following way. In this model the released stress is distributed non-uniformly and the share amount received by an intact fiber depends inversely to some power of the distance of separation from the broken fiber [13]. A number of other processes have been studied in the framework of fiber bundle models. For example, how the damage evolves due to an environmentally assisted aging process in a fiber bundle model has been studied in [14]. In this paper, we study the breakdown properties of the fiber bundles with ELS dynamics.

Let  $\sigma$  be the uniform applied load per fiber initially when all fibers are intact. The total amount of external

load is then  $F = N\sigma$ . This externally applied load gets distributed within the bundle in a series of  $T$  successive time steps. Let us denote  $x_t$  as the stress per intact fiber after  $t$ -th relaxation step. Since more and more fibers break, the stresses acting through the remaining intact fibers increase. When  $\sigma$  is the applied load per fiber, all fibers with  $b_i < \sigma$  break. This stress is now distributed to  $N[1 - P(\sigma)]$  intact fibers on the average. After the first step if  $x_1$  is the stress per fiber then  $F = Nx_1[1 - P(\sigma)]$ . Consideration of the same mechanism in successive steps one can write:

$$F = Nx_1[1 - P(\sigma)] = Nx_2[1 - P(x_1)] = Nx_3[1 - P(x_2)].. \quad (1)$$

This process terminates after  $T$  steps when the amount of stress released is not sufficient to create further failure of fibers.

If  $x$  is the applied load per intact fiber in the stable state, then one can write the external load  $F(x)$  as a function of  $x$ , which is  $F(x) = Nx[1 - P(x)]$  [6, 15]. For a specific value of  $x = x_c$ ,  $F(x)$  is maximum which suggests the condition:  $1 - P(x_c) - x_cp(x_c) = 0$ . For example, for a uniform distribution of breaking thresholds one gets  $\sigma_c = F_c/N = 1/4$  [15].

The failure properties of materials are highly dependent on the extent of disorder inherent in them. In the FBMs, this disorder appears in the breaking thresholds of the individual fibers. In this regard, the power law distribution of breaking thresholds is an extreme case of heterogeneous disorder, where a large number of fibers have very small breaking thresholds, their numbers decreases as breaking thresholds are increased, leading to few fibers with large breaking thresholds. It is already known in the literature that the probability of getting a warning of imminent breakdown of the system is higher when the material is more heterogeneous [16]. Such cases of extremely heterogeneous disorder has not been very well studied in the literature of fiber bundle model. Another form of strong heterogeneity has been studied where a fraction of fibers are completely unbreakable and the breaking thresholds of the rest are drawn from some distribution [17, 18]. In this paper we therefore address the problem of FBMs with highly heterogeneous power law distributed breaking thresholds of individual fibers. As a first step we study the simpler problem of ELS dynamics in this model, study of the LLS version will be taken up in a future publication.

FBMs have a wide variety of applications. It is a versatile tool to understand conceptually the underlying microscopic mechanism of fatigue [19], failure of composite materials [20], landslides [21] etc. Moreover, the ELS version of the FBM studied here may be used to study the traffic jams in roads [22]. The traffic flow capacities of the roads can be mapped to the breaking thresholds of individual fibers. The highly disorder flow rates may occur in a traffic network with few highways and a large

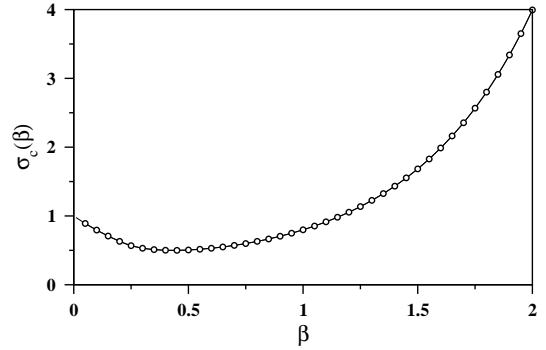


FIG. 1: The initial external load  $\sigma_c(\beta)$  per fiber given in Eqn. 5 (solid line) matches excellently with its numerical estimates (open circles).

number of narrow roads connecting the highways.

In section 2 we describe our study of the fiber bundle model with power law distributed breaking thresholds. We also describe different analytically obtained results characterizing this bundle and their numerical supports. In section 3 the statistics of avalanche size distribution have been described. We summarize in section 4.

## 2. HIGHLY DISORDERED FIBER BUNDLES

In this paper we report the results of our study of the breakdown properties of a fiber bundle where the breaking thresholds of the individual fibers are power law distributed. As in other FBMs, the only source of disorder in our model is the random distribution of breaking thresholds. Therefore, the individual breaking thresholds  $b_i$  are drawn from a probability distribution  $p(b) \sim b^{-\gamma}$  with  $\gamma = 1$ . Initially  $N$  uniformly distributed random numbers  $q_i$  are drawn within  $-1 < q_i < 1$  and the breaking threshold  $b_i = 10^{\beta q_i}$  for the  $i$ -th fiber is assigned. Consequently, the probability distribution takes the form  $p(b) \sim b^{-1}$  within the range  $10^{-\beta}$  to  $10^{\beta}$  [16].

Here, we use the same formulation described in section 1 to obtain the breaking strength of the bundle  $\sigma_c$  as a function of the cut-off parameter  $\beta$  when the breaking thresholds  $\{b_i\}$  are power law distributed. The constant of proportionality can be evaluated from the normalization condition, which gives the functional form  $p(b) = b^{-1}/(2\beta \ln 10)$ . As a result, the cumulative probability distribution is given by,

$$P(b) = \int_{10^{-\beta}}^b p(z) dz = \ln b / (2\beta \ln 10) + 1/2. \quad (2)$$

In this case we obtain the expression of  $F(x)$  as

$$F(x) = Nx[1/2 - \ln x / (2\beta \ln 10)]. \quad (3)$$

Clearly the function  $F(x)$  has a maximum at  $x = x_c$  for which  $dF(x)/dx = 0$ . This yields  $x_c = 10^{\beta}/e$

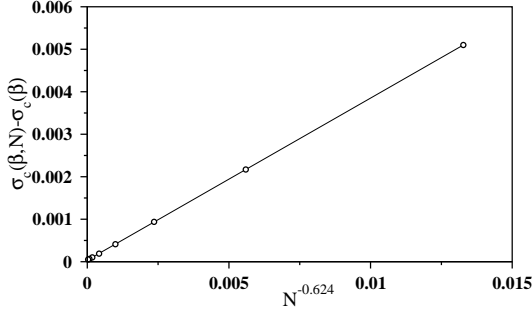


FIG. 2: Variation of the critical load  $\sigma_c(\beta, N)$  on the system size  $N$  for  $\beta = 0.225$  has been exhibited. Plot of  $\sigma_c(\beta, N) - \sigma_c(\beta)$  vs.  $N^{-0.624}$  with  $\sigma_c(\beta) = 0.596$  shows a nice straight line that passes very close to the origin.

and the total critical applied load is  $F_c \equiv F(x_c) = N10^\beta/(2\beta e \ln 10)$ . Thus the critical initial applied load per fiber is given by

$$\sigma_c(\beta) = F_c/N = 10^\beta/(2\beta e \ln 10). \quad (4)$$

Let  $b^*$  denote the minimum of the breaking thresholds. Since the definition of  $x_c$  signifies that a bundle fails completely at this point then, the condition  $b^* = x_c$  i.e.,  $10^{-\beta} = 10^\beta/e$  fixes the upper bound of  $\beta$  denoted as  $\beta_u = 1/(2 \ln 10)$  for which the weakest fiber failure leads to the complete breakdown of the bundle. Thus we have the complete expression for  $\sigma_c(\beta)$ :

$$\sigma_c(\beta) = \begin{cases} 10^\beta/(2e \ln 10^\beta) & \text{for } \beta \geq \beta_u \\ 10^{-\beta} & \text{for } \beta \leq \beta_u \end{cases} \quad (5)$$

The above expression for the average critical applied load per fiber  $\sigma_c(\beta)$  for a given value of cut-off parameter  $\beta$  is valid only for infinitely large bundles, i.e.,  $N \rightarrow \infty$ .

The width of the distribution of breaking thresholds increases with  $\beta$  and the critical threshold  $\sigma_c(\beta)$  varies accordingly. For  $\beta = 0$ , all fibers have the same breaking thresholds equal to unity and therefore  $\sigma_c(0) = 1$ . When  $\beta$  is small, the minimum breaking threshold is high enough, and very close to unity. When the external stress per fiber is raised to reach the minimum breaking threshold, it breaks. The released stress is distributed among the remaining fibers and is sufficient to break all other fibers. This mechanism, when failure of the weakest fiber ensures the global failure of the entire bundle is analogous to the brittle fracture. This situation continues till  $\beta$  reaches  $\beta_u$  and therefore  $\sigma_c(\beta)$  decreases as the strength of the weakest fiber, i.e.,  $10^{-\beta}$ . When  $\beta$  increases further, gradually fibers of high breaking thresholds appear and they take over the control. Consequently,  $\sigma_c(\beta)$  must increase with  $\beta$  for large  $\beta$  with a minimum at  $\beta = \beta_m$ . The value of  $\beta_m$  is obtained using the condition  $d\sigma_c(\beta)/d\beta = 0$  in Eqn. (5) at  $\beta_m = 1/(\ln 10)$ , which is twice the value of  $\beta_u$ .

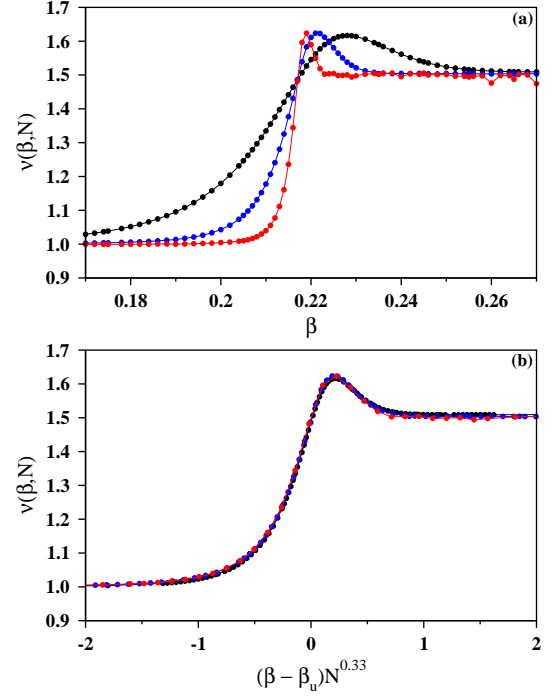


FIG. 3: (Color online) (a) Plot of  $\nu(\beta, N)$  vs  $\beta$  for systems of different sizes. The value of  $\nu(\beta, N)$  calculated using the four bundle sizes from  $N = 2^{10}$  to  $2^{16}$  (black),  $2^{14}$  to  $2^{20}$  (blue) and  $2^{18}$  to  $2^{24}$  (red);  $N$  is increased from left to right. (b) A collapse of the data of the same three system sizes works excellent when the  $\beta$  axis has been suitably scaled.

Numerically  $\sigma_c(\beta)$  is obtained in the following way. For a given value of  $\beta$  we first calculate the critical load per fiber  $\sigma_c^\alpha(\beta, N)$  for a particular fiber bundle  $\alpha$  having  $N$  fibers with a given set of breaking thresholds  $\{b_i\}$ . This calculation is repeated over a large number of uncorrelated bundles  $\alpha$  and their critical loads are averaged to obtain  $\sigma_c(\beta, N) = \langle \sigma_c^\alpha(\beta, N) \rangle$ . The entire calculation is then repeated for different values of  $N$ .

To obtain  $\sigma_c^\alpha(\beta, N)$ , the breaking thresholds are arranged in increasing order ( $b_{(1)}^\alpha < b_{(2)}^\alpha < b_{(3)}^\alpha < \dots < b_{(N)}^\alpha$ ). The bundle will support the initially applied load per fiber ( $\sigma$ ) if  $\sigma < b_{(1)}^\alpha$  or  $\sigma N/(N-1) < b_{(2)}^\alpha$  or  $\sigma N/(N-2) < b_{(3)}^\alpha$  or ...  $\sigma N < b_{(N)}^\alpha$ . If all these inequalities fail to satisfy then the bundle will no longer support the load, it will break apart. Now if  $\sigma$  is such that it is sufficient to break  $n$  fibers, then at this stage the bundle will support the load if  $\sigma N/(N-n) < b_{(n+1)}^\alpha$  i.e.,

$$\sigma < [(N-n)/N]b_{(n+1)}^\alpha. \quad (6)$$

The term in the parenthesis of Eqn. (6) decreases with  $n$  and  $b_{(n+1)}^\alpha$  is an increasing function of  $n$  as thresholds are arranged in increasing order. So, the function at the right hand side of Eqn. (6) has a maximum at some  $n$  and if the  $\sigma$  is raised at this maximum value,

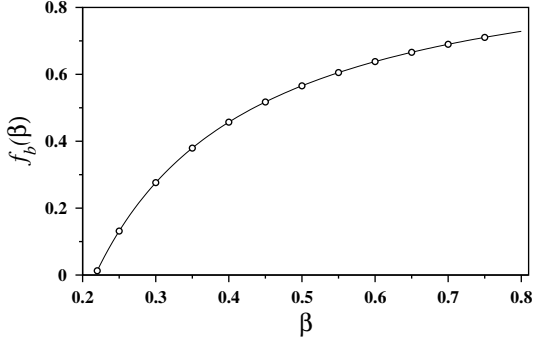


FIG. 4: Plot of the fraction of broken fibers  $f_b(\beta)$  for a particular value of  $\beta$  right before the complete breakdown of the bundle is plotted for the analytical expression given in Eqn. 9 with solid line. The numerically obtained data represented by open circles matches very well with the analytical curve.

the bundle will break immediately. So the maximum of  $[(N - n)/N]b_{(n+1)}^\alpha$  determines the critical load per fiber for the bundle  $\alpha$ . Therefore [23],

$$\sigma_c^\alpha(\beta, N) = \max \left\{ b_{(1)}^\alpha, \frac{N-1}{N} b_{(2)}^\alpha, \frac{N-2}{N} b_{(3)}^\alpha, \dots, \frac{1}{N} b_{(N)}^\alpha \right\} \quad (7)$$

We now assume that the average value of the critical load per fiber  $\sigma_c(\beta, N)$  for a given value of  $\beta$  and for the bundle of size  $N$  converges to a specific value  $\sigma_c(\beta)$  as  $N \rightarrow \infty$  according to the following form:

$$\sigma_c(\beta, N) - \sigma_c(\beta) = AN^{-1/\nu(\beta)} \quad (8)$$

where  $\nu(\beta)$  is a critical exponent for the cut-off parameter  $\beta$ . We have plotted  $\sigma_c(\beta, N)$  against  $N^{-1/\nu(\beta)}$  for  $N = 2^{18}$  to  $2^{24}$ ,  $N$  being increased by a factor of 4 at each stage. For a particular value of  $\beta$  we have used different trial values of  $\nu(\beta)$  so that for a specific value of  $\nu(\beta)$  the plot fits (by least square fit) to the best straight line. Using this best value of  $\nu(\beta)$  and on extrapolation to  $N \rightarrow \infty$  we obtained  $\sigma_c(\beta)$ . In Fig. 1 we have exhibited an excellent matching of the analytical and the numerical values of  $\sigma_c(\beta)$  for the range  $0 < \beta \leq 2$ .

We now investigate the dependence of the finite size correction exponent  $\nu(\beta)$  on the cut-off parameter  $\beta$ . We recall that in the case of a uniform breaking threshold distribution, the plot of  $\sigma_c(N) - \sigma_c$  as a function of  $N^{-1/\nu}$  gives an excellent straight line with  $\sigma_c = 1/4$  and  $\nu = 3/2$  [24–27]. Similarly, for our model of highly disordered FBM, the plot of  $\sigma_c(\beta, N) - \sigma_c(\beta)$  against  $N^{-1/\nu(\beta)}$  is carried out for different values of  $\beta$ . For example, we obtain the best possible value of  $\nu(\beta)$  to be 1.603 for  $\beta = 0.225$  shown in Fig. 2. In this way the critical exponent  $\nu(\beta)$  is calculated for different  $\beta$  and its variation is shown in Fig. 3(a) using  $N = 2^{10}$  to  $2^{16}$ ,  $2^{14}$  to  $2^{20}$  and  $2^{18}$  to  $2^{24}$ . The value of  $\nu(\beta)$  first increases, attains a maximum value  $\approx 1.63$ , then decreases and saturates to 1.5 with

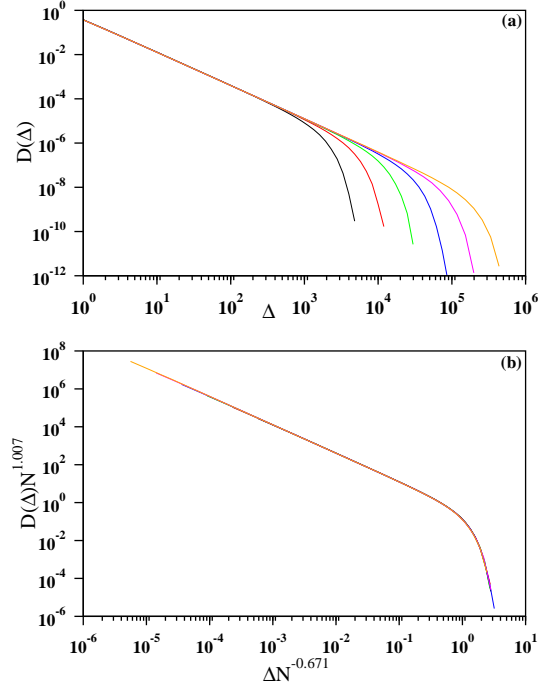


FIG. 5: (Color online) (a) Log-log plot of the binned data for avalanche size distribution  $D(\Delta)$  vs  $\Delta$  for  $\beta = \beta_u = 1/(2 \ln 10)$  for  $N = 2^{16}$ ,  $N = 2^{18}$  ...  $2^{26}$  (from left to right). (b) A finite-size scaling works well:  $D(\Delta)N^\eta$  against  $\Delta N^{-\zeta}$  exhibits a good collapse of data with  $\eta = 1.007$  and  $\zeta = 0.671$  implying  $\xi = \eta/\zeta = 1.50(1)$ . This value is consistent with the directly measured value of 1.50(2) from the slopes in the intermediate region. The crossover is not observed here since  $\Delta_c = \infty$  for this particular value of  $\beta$ .

further increment of  $\beta$ . The same data in Fig. 3(a) when plotted against  $(\beta - \beta_u)N^{0.33}$  shows a good collapse as shown in Fig. 3(b). Thus we conclude that the curve for  $\nu(\beta)$  retains its nature for large bundle sizes.

Next we calculate the fraction of broken fibers  $f_b(\beta)$  just before complete breakdown of the bundle as a function of the cut-off parameter  $\beta$ . Since at  $x_c$  the fiber bundle fails completely, so the quantity  $f_b(\beta)$  is calculated as:

$$f_b(\beta) = \int_{10^{-\beta}}^{x_c} p(x) dx = 1 - 1/(2\beta \ln 10). \quad (9)$$

As the fraction of broken fibers  $f_b(\beta)$  is a positive quantity thus the condition  $1 - 1/(2\beta \ln 10) > 0$  again reproduces the result that for  $\beta < 1/(2 \ln 10)$  the weakest element failure leads to the catastrophic breakdown of the bundle.

Numerically  $f_b(\beta)$ , for a given value of  $\beta$  is calculated in the same way as described previously in the case of  $\sigma_c(\beta)$ . The external load is increased quasi-statically until the bundle fails. Just before complete breakdown of the bundle, the fraction of broken fibers is calculated for a particular  $N$  and averaged over large number of sam-

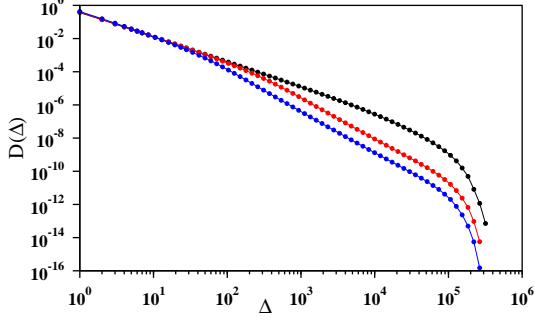


FIG. 6: (Color online) The avalanche size distribution for  $\beta = 0.22$  (black),  $0.24$  (red) and  $0.28$  (blue) (from right to left) for bundles of size  $N = 2^{24}$ . Slopes of the curve are  $\approx 1.5$  and  $\approx 2.5$  for small and large avalanche sizes. The crossover size  $\Delta_c(\beta)$  are approximately 11741, 200.4 and 31.66 respectively evaluated using Eqn. 17.

ples to obtain  $f_b(\beta, N)$ . Then this procedure is repeated for six values of  $N = 2^{16}, 2^{18}, \dots, 2^{26}$  and an extrapolation on  $f_b(\beta, N)$  as  $N \rightarrow \infty$  yields  $f_b(\beta)$ . In Fig. 4 the numerically obtained results are compared with the analytical one, indicating a good agreement.

### 3. AVALANCHE SIZE DISTRIBUTION

In a stable fiber bundle, the stress acting through every intact fiber is less than its breaking threshold. Now, if the externally applied load is suitably raised so that it becomes equal to the breaking threshold of the weakest fiber, then this fiber breaks. This triggers a cascade of fiber failures which finally ends when the bundle attains a new stable state. The total number  $\Delta$  of fibers that fail in this event is called the avalanche size. Starting from a completely intact fiber bundle the global failure of the entire bundle may be attained by raising the external load in such a quasi-static process, causing a series of avalanches. The probability distribution  $D(\Delta)$  is regarded as an interesting quantity to study. It is well known that for the uniform distribution of breaking thresholds of individual fibers and for the ELS dynamics, the probability distribution is a power law [28]

$$D(\Delta) \sim \Delta^{-\xi}, \quad (10)$$

with  $\xi = 5/2$ . In the following we would see that in our case of power law distributed breaking thresholds the exponent  $\xi$  undergoes a crossover from  $3/2$  to  $5/2$ .

To exhibit the crossover behavior we follow the method in [29]. For a bundle having large number of fibers, the number of avalanches of size  $\Delta$  is given by [28]

$$\frac{D(\Delta)}{N} = \frac{\Delta^{\Delta-1} e^{-\Delta}}{\Delta!} \int_0^{x_c} p(x) r(x) [1 - r(x)]^{\Delta-1} e^{\Delta r(x)} dx, \quad (11)$$

where,

$$r(x) = 1 - \frac{xp(x)}{1 - P(x)}. \quad (12)$$

The expression for  $D(\Delta)$  can be simplified to the following form [29]:

$$\frac{D(\Delta)}{N} = \frac{\Delta^{\Delta-2} e^{-\Delta}}{\Delta!} \frac{p(x_c)}{|r'(x_c)|} (1 - e^{-\Delta/\Delta_c}), \quad (13)$$

with

$$\Delta_c = \frac{2}{r'(x_c)^2 (x_c - b^*)^2}. \quad (14)$$

Using the Stirling approximation  $\Delta! = \Delta^\Delta e^{-\Delta} \sqrt{2\pi\Delta}$ , Eqn. (13) can be written as

$$\frac{D(\Delta)}{N} = C \Delta^{-5/2} (1 - e^{-\Delta/\Delta_c}), \quad (15)$$

Where  $C = (2\pi)^{-1/2} p(x_c)/|r'(x_c)|$  is a constant. From Eqn. (15), a clear evidence of crossover in the exponent  $\xi$  around the avalanche size  $\Delta_c$  is prominent. So we have:

$$\frac{D(\Delta)}{N} \propto \begin{cases} \Delta^{-3/2} & \text{for } \Delta \ll \Delta_c, \\ \Delta^{-5/2} & \text{for } \Delta \gg \Delta_c. \end{cases} \quad (16)$$

In our case, we use power law distribution  $p(b) \sim b^{-1}$  in the range from  $10^{-\beta}$  to  $10^\beta$  to obtain  $r'(x_c) = -e/10^\beta$ ,  $x_c = 10^\beta/e$  and  $b^* = 10^{-\beta}$ . Substituting these values in Eqn. (14) we get the crossover avalanche size:

$$\Delta_c(\beta) = \frac{2}{(1 - e10^{-2\beta})^2}. \quad (17)$$

This crossover phenomenon has also been studied using numerical simulations. For  $\beta = 1/(2 \ln 10)$  Eqn. (17) yields  $\Delta_c = \infty$ . Thus only the  $\xi = 3/2$  power law is observed as any avalanche of finite size  $\Delta$  is less than the value of  $\Delta_c$  at this particular value of  $\beta$ . In Fig. 5(a), the numerical data for the avalanche size distribution for  $\beta = 1/(2 \ln 10)$  has been plotted for six different values of  $N$  starting from  $N = 2^{16}$  to  $2^{26}$ ;  $N$  being increased by a factor of 4 at each stage. For  $N = 2^{16}$  to  $2^{22}$  the data has been averaged over  $10^6$  samples and 400000 and 100000 samples for  $2^{24}$  and  $2^{26}$  respectively. A finite-size scaling has also been done in Fig. 5(b) by use of suitable powers of the bundle size  $N$ . This indeed exhibits an excellent data collapse confirming the following scaling form:

$$D(\Delta) N^\eta \sim \mathcal{G}[\Delta/N^\zeta] \quad (18)$$

where  $\mathcal{G}(y)$  is an universal scaling function of the scaled variable  $y = \Delta/N^\zeta$ . The best possible tuned values of the scaling exponents obtained are  $\eta = 1.007$  and  $\zeta = 0.671$ . Using these scaling exponents the value of  $\xi = \eta/\zeta =$

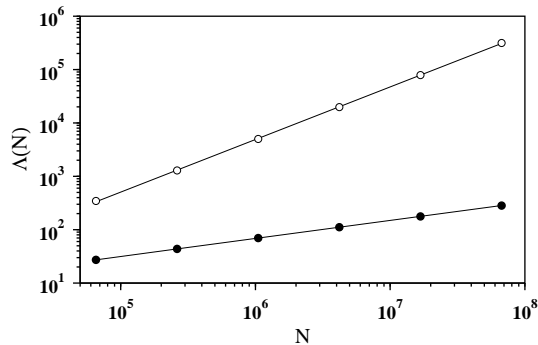


FIG. 7: Plot of the average number of avalanches  $\Lambda(N)$  required to break the bundle of size  $N$  on a log-log scale: for  $\beta = 1/(2 \ln 10)$ ,  $\Lambda(N) \sim N^{0.337}$  (filled circles) and for  $\beta = 0.240$ ,  $\Lambda(N) \sim N^{0.985}$  (open circles).

1.50(1) is calculated, which is a very well tally with the analytical result of  $3/2$ .

We have also tried the same analysis for  $\beta = 0.22, 0.24$  and  $0.28$ . Using Eqn. (17) we have obtained  $\Delta_c(\beta) = 11741, 200.4$  and  $31.66$  respectively. A clear evidence of the crossover in the exponent  $\xi$  around  $\Delta = \Delta_c(\beta)$  is observed as shown in Fig. 6 for  $N = 2^{24}$ . The slope of the curve gradually crosses over from  $\approx 1.5$  to  $\approx 2.5$  for large values of  $\Delta$ . It has also been observed that as  $\beta$  is increased,  $\Delta_c(\beta)$  gradually shifts towards the origin and therefore the regime over which  $\xi = 5/2$  is valid, gets extended. Such a crossover has been observed earlier in [29, 30] for the FBM with uniform distribution of breaking thresholds ranged between a certain lower cut-off  $b_{lc}$  and unity. Here, avalanche sizes smaller (larger) than some crossover size  $\Delta(b_{lc})$  correspond to avalanche size exponents  $3/2$  ( $5/2$ ). This implies that in our model, even for the highly heterogeneous distribution of breaking thresholds, similar crossover between the same two exponents takes place across the crossover avalanche size  $\Delta_c(\beta)$ .

It has also been observed that the total number of avalanches  $\Lambda(N)$  depends on the system sizes  $N$  as  $N^\chi$ , where  $\chi = 0.336$  and  $0.985$  for  $\beta = 1/(2 \ln 10)$  and  $0.240$  respectively. The log-log plot of  $\Lambda(N)$  against  $N$  for these two values of  $\beta$  fits to excellent straight lines as shown in Fig. 7. We conjecture that  $\chi$  may be  $1/3$  and  $1$  exactly for  $\beta = \beta_u$  and  $\beta > \beta_u$  respectively.

#### 4. SUMMARY

Properties of the fiber bundle model have been studied using equal load sharing dynamics where the breaking thresholds of the fibers have been assigned from a power law distribution  $p(b) \sim b^{-1}$  in the range from  $10^{-\beta}$  to  $10^\beta$ . Variations of different quantities characterizing the bundle have been studied with the cut-off exponent  $\beta$ .

The critical external load per fiber  $\sigma_c(\beta)$  required for the global breakdown of the bundle as well as the fraction  $f_b(\beta)$  of broken fibers right before it are estimated both analytically as well as numerically, and a good correspondence has been observed. For very small and very high values of  $\beta$  the breaking strength of only a single fiber determines the critical strength of the entire bundle. For example, for very small  $\beta$ , it is enough to tune the external load to the strength of the weakest fiber which then triggers a large avalanche and the entire bundle fails, implying  $\sigma_c(\beta) = 10^{-\beta}$ . Such a behavior continues till  $\beta = \beta_u$  and this regime is analogous to the brittle failure of materials. When  $\beta$  is raised beyond  $\beta_u$ , equating the external load to the strength of the weakest fiber is no more sufficient for the global failure, the large number of fibers with breaking thresholds near the minimum still dominate. Consequently the number of avalanches required for the breakdown of the bundle gradually increases and the  $\sigma_c(\beta)$  slowly increases from the weakest strength of  $10^{-\beta}$  but for  $\beta > \beta_u$ ,  $\sigma_c(\beta)$  remains smaller than  $10^{-\beta_u}$ . Therefore, a minimum in  $\sigma_c(\beta)$  is reached at  $\beta_m = 2\beta_u$  and from this point,  $\sigma_c(\beta)$  starts increasing. As a result,  $\sigma_c(\beta)$  becomes equal to  $10^{-\beta_u}$  again and then increases indefinitely. For very large  $\beta$  the external load must be raised to  $\sigma_c(\beta) \approx 10^\beta$  to break the strongest fiber of breaking threshold around  $10^\beta$ . This salient feature is a direct consequence of the power law distribution of the breaking thresholds.

More interestingly, we have also shown numerically that the critical load  $\sigma_c(\beta, N)$  approaches its asymptotic value as  $\sigma_c(\beta, N) = \sigma_c(\beta) + AN^{-1/\nu(\beta)}$ . The finite size correction exponent  $\nu(\beta)$  is first seen to increase sharply with  $\beta$ , reaches a maximum, then decreases and finally converges to a value  $\approx 3/2$ . Statistical analysis of the avalanche sizes have been done. The avalanche size distribution follows a power law and the associated exponent  $\xi$  crosses over from  $3/2$  to  $5/2$  through a crossover avalanche size  $\Delta_c(\beta)$ .

#### ACKNOWLEDGEMENT

We thankfully acknowledge Alex Hansen for suggesting this problem and many useful discussions.

---

\* Electronic address: manna@bose.res.in

- [1] H. J. Herrmann and S. Roux, *Statistical Models for the Fracture of Disordered Media*, Elsevier, Amsterdam, 1990.
- [2] B. K. Chakrabarti and L. G. Benguigui, *Statistical Physics of Fracture and Breakdown in Disordered Systems*, Oxford University Press, Oxford, 1997.
- [3] D. Sornette, *Critical Phenomena in Natural Sciences*, Springer-Verlag, Berlin, 2000.

- [4] M. Sahimi, *Heterogenous Materials II: Nonlinear and Breakdown Properties*, Springer-Verlag, New York, 2003.
- [5] P. Bhattacharya and B. K. Chakrabarti, *Modelling Critical and Catastrophic Phenomena in Geoscience*, Springer-Verlag, Berlin, 2006.
- [6] S. Pradhan, B. K. Chakrabarti and A. Hansen, Rev. Mod. Phys., **82**, 499 (2010).
- [7] F. T. Pierce, J. Text. Inst., **17**, T355 (1926).
- [8] H. E. Daniels, Proc. R. Soc. Lond. A, **183**, 405 (1945).
- [9] J. V. Andersen, D. Sornette and K. Leung, Phys. Rev. Lett. **78**, 2140 (1997).
- [10] M. Kloster, A. Hansen and P. C. Hemmer, Phys. Rev. E., **56**, 2615 (1997).
- [11] D. G. Harlow and S. L. Phoenix, Int. J. Fract., **17**, 601 (1981).
- [12] D. G. Harlow and S. L. Phoenix, J. Mech. Phys. Solids, **39**, 173 (1991).
- [13] R. C. Hidalgo, Y. Moreno, F. Kun, and H. J. Herrmann, Phys. Rev. E, **65**, 046148 (2002).
- [14] S. Lennartz-Sassinek, I. G. Main, Z. Danku and F. Kun, Phys. Rev. E, **88**, 032802 (2013).
- [15] S. Pradhan and P. C. Hemmer, Phys. Rev. E, **75**, 056112 (2007).
- [16] A. A. Moreira, C. L. N. Oliveira, A. Hansen, N. A. M. Araujo, H. J. Herrmann and J. S. Andrade, Jr., Phys. Rev. Lett., **109**, 255701 (2012).
- [17] R. C. Hidalgo, K. Kovacs, I. Pagonabarraga and F. Kun, Eur. Phys. Lett., **81**, 54005 (2008).
- [18] K. Kovacs, R. C. Hidalgo, I. Pagonabarraga and F. Kun, Phys. Rev. E, **87**, 042816 (2013).
- [19] W. A. Curtin, J. Am. Ceram. Soc. **74**, 2837 (1991).
- [20] F. Kun, M. H. Costa, R. N. Costa Filho, J. S. Andrade, J. B. Soares, S. Zapperi, and H. J. Herrmann, J. Stat. Mech.: Theory Exp., P02003 (2007).
- [21] D. Cohen, P. Lehmann and D. Or, Water Resour. Res., **45**, W10436 (2009).
- [22] B. K. Chakrabarti, Physica A **372**, 162 (2006).
- [23] R. L. Smith and S. L. Phoenix, ASME J. Appl. Mech., **48**, 75 (1981).
- [24] C. Roy, S. Kundu and S. S. Manna, Phys. Rev. E, **67**, 062137 (2013).
- [25] R. L. Smith, Ann. Prob., **10**, 137 (1982).
- [26] L. N. McCartney and R. L. Smith, ASME J. Appl. Mech., **50**, 601 (1983).
- [27] H. E. Daniels and T. H. R. Skyrme, Adv. Appl. Probab., **21**, 315 (1989).
- [28] P. C. Hemmer and A. Hansen, J. Appl. Mech., **59**, 909 (1992).
- [29] S. Pradhan, A. Hansen and P. C. Hemmer, Phys. Rev. E, **74**, 016122 (2006).
- [30] S. Pradhan, A. Hansen and P. C. Hemmer, Phys. Rev. Lett., **95**, 125501 (2005).